The Astrophysical Journal, 395:113–118, 1992 August 10

DYNAMICAL EVOLUTION OF HIGHLY INCLINED RINGS

Dimitris M. Christodoulou,[1,2] Neal Katz,[1,3] Hans-Walter Rix,[1,4] and Asao Habe[5]

Received 1991 November 6; accepted 1992 February 14

ABSTRACT

We have used three computer programs (two smoothed-particle hydrodynamics codes and one Eulerian hydrodynamics code) to model the detailed dynamical evolution of gaseous rings inside external spheroidal potential wells. In this paper, we discuss rings highly inclined to the equatorial symmetry plane; this is relevant to polar rings observed around galaxies. Our primary objective is to clarify the possible evolution of the rings because, in the past, different numerical techniques have produced entirely different scenarios. We find that the evolution is not affected by the magnitude or type of viscosity but can be strongly dependent on the adopted initial conditions. Our main conclusion is that real polar rings are *not* expected to collapse into the nuclear region or to settle significantly toward the preferred equatorial orientation within one Hubble time unless the shapes of the surrounding halos are either extremely distorted or distinctly prolate.

Subject headings: galaxies: evolution — galaxies: kinematics and dynamics — hydrodynamics

1. INTRODUCTION

The basic questions associated with the existence of highly inclined ("polar") rings around galaxies concern the processes that affect their long-term evolution and the mechanisms that may allow them to survive for at least one Hubble time (Schechter & Gunn 1978; Steiman-Cameron & Durisen 1982; Athanassoula & Bosma 1985; Tohline 1990; Whitmore et al. 1990; Steiman-Cameron 1991). To investigate these questions within the general context of evolving inclined gaseous disks, we have undertaken a comparative study of hydrodynamical models that evolve from diverse initial conditions inside external potential wells. We have used three different computer programs for this study: two based on smoothed particle hydrodynamics (SPH), the code developed by Habe & Ikeuchi (1985), and the TREESPH code developed by Hernquist & Katz (1989); and the Eulerian hydro code used by Christodoulou & Tohline (1991). Hydrodynamical evolution of several models is described and discussed in detail elsewhere (e.g., Habe & Ikeuchi 1985, 1988; Christodoulou 1989, 1990; Christodoulou & Tohline 1991, 1992; Rix & Katz 1991; Katz & Rix 1992a, b). Below we discuss only results that concern highly inclined, massless rings that evolve inside static, spheroidal potential wells.

The problem with understanding the detailed evolution of highly inclined rings is that different numerical techniques have produced different results (compare the results of Habe & Ikeuchi 1985; Varnas 1986a, b, 1990; Steiman-Cameron & Durisen 1988; Christodoulou 1990; Quinn 1991a; Katz & Rix 1992a, b). Furthermore, some studies (see § 2 below) are in complete disagreement with theoretical predictions (Tohline & Durisen 1982; Tohline, Simonson, & Caldwell 1982; Durisen et al. 1983; Steiman-Cameron & Durisen 1984). According to theory, highly inclined rings in static, spheroidal potentials are expected to precess differentially only *slowly* and, as a result of dissipation, to settle *slowly* toward the equatorial plane of the potential; they are transient but extremely long-lived structures.

In § 2, we briefly describe the available results from hydrodynamical modeling of highly inclined ($\sim 80°$) rings. In all the models, c is the symmetry axis of the potential and the inclination angle is measured from the symmetry plane defined by the a and b axes. In § 3, we analyze the difference between models evolved in oblate and prolate potentials and discuss the effects of using different initial conditions and viscosity prescriptions in the hydro codes. Finally, in § 4, we summarize the four possible evolutionary scenarios for which we have reached a concensus.

2. SUMMARY OF HYDRODYNAMICAL MODELS

In this section we describe previous and new hydrodynamical computations of highly inclined rings evolving inside external potential wells. The most important characteristics and model parameters are listed in Table 1. The models at the bottom of the table are new and were computed for the purposes of this paper. Table 1 should serve as a guide to the reader for the subsequent discussion.

2.1. *Previous Work*

Habe & Ikeuchi (1985) used an SPH code to compute the evolution of a highly inclined ring inside a prolate spheroidal potential with an axis ratio $c/a = 1.33$ (model 1 in Table 1). They found that the ring attempted to settle, but after 1/4 of a precession period it began to disrupt and finally collapsed into the nucleus after about one precession period. Steiman-Cameron & Durisen (1988) used a cloud-fluid code to simulate the settling process from low and moderate inclinations. They predicted that at high inclinations the evolution time scales would be much longer and that inflow would be more important than at lower inclinations. Along similar lines, Varnas (1990), using his SPH code, found that settling from high inclinations proceeded at a slower pace and that nuclear inflow increased (model 2). Christodoulou (1990) used an Eulerian hydro code to evolve a highly inclined torus inside an oblate potential with $c/a = 0.95$ (models 3). In contrast to the above results, the torus remained close to its original position for about 30 rotations, while settling and inflow remained very

[1] Steward Observatory, University of Arizona, Tucson, AZ 85721.
[2] Harvard-Smithsonian Center for Astrophysics, 60 Garden Street, Cambridge, MA 02138.
[3] Department of Physics, MIT 6-214, Cambridge, MA 02139.
[4] Institute for Advanced Study, School of Natural Sciences, Princeton, NJ 08540.
[5] Department of Physics, Hokkaido University, Sapporo 060, Japan.

TABLE 1

HYDRODYNAMICAL MODELS

			Potential		Initial Conditions				Physical Conditions				
No.	Reference	Code[a]	Type	c/a[b]	Initial Model[c]	i[d]	$\Delta r/r$[e]	τ_p/τ_o[f]	n[g]	Viscosity[h]	Self-Gravity[i]	Cooling	Result
1	Habe & Ikeuchi 1985	SPH	Scale-free logarithmic	1.33	Flat ring	80°	0.33	23	∞	Artifical	No	No	Collapse to nucleus
2	Varnas 1990	SPH	Schwarzschild	...	Flat ring	70°	0.67	53	...	Artificial	No	No	Nuclear inflow and settling
3	Christodoulou 1990	EH	Homogeneous spheroid	0.95	Torus	80°	0.50 0.25	192	1.5	Numerical	No	No	Torus remains close to original orientation
4	Christodoulou & Tohline 1992	EH	Homogeneous spheroid	0.71	Torus	80°	0.50 0.25	20	1.5	Numerical	No	No	Abrupt attempt to settle, inflow dominates
5	Katz & Rix 1992a..........	TREESPH	Scale-free logarithmic	0.90 0.75	Flat ring	80°	0.10	53 19	1.5	Artificial	No/Yes	Yes	Warped pseudo-equilibrium at high inclination
6	Katz & Rix 1992a..........	TREESPH	Scale-free logarithmic	0.90 0.75	Flat ring	80°	0.10	53 19	1.5	Artificial	No/Yes	No	Collapse to nucleus
7	Katz & Rix 1992b..........	TREESPH	Scale-free logarithmic	0.90 0.75	Gaseous satellite	80°	0.13	53 19	1.5	Artificial	No/Yes	Yes	Warped pseudo-equilibrium at high inclination
8	Quinn 1991b	STICKY	Scale-free logarithmic	0.75	Flat ring	80°	0.10	19	...	Clouds	No	Yes	Ring remains close to original orientation
9	Quinn 1991b	STICKY	Scale-free logarithmic	1.33	Flat ring	80°	0.10	23	...	Clouds	No	Yes	Collapse to nucleus
10	This paper	TREESPH	Scale-free logarithmic	1.33	Flat ring	80°	0.10	23	1.5	Artificial	No	Yes/No	Collapse to nucleus
11	This paper	EH	Homogeneous spheroid	1.33	Torus	80°	0.50	25	1.5	Numerical	No	No	Collapse to nucleus
12	This paper	SPH	Scale-free logarithmic	0.95	Flat ring	80°	0.33	110	∞	Artificial	No	No	Ring remains close to original orientation
13	This paper	SPH	Scale-free logarithmic	1.11	Flat ring	80°	0.33	57	∞	Artificial	No	No	Collapse to nucleus
14	This paper	EH	Scale-free logarithmic	0.90 0.75	Flat ring	80°	0.10	53 19	1.5	Numerical	No	No	Collapse to nucleus

[a] SPH denotes the codes of Varnas and Habe & Ikeuchi. TREESPH denotes the code of Hernquist & Katz. EH denotes the grid-based Eulerian hydro code of Tohline & Christodoulou. STICKY denotes the "sticky-particle" code of Quinn.
[b] Axis ratio of the spheroidal potential.
[c] Flat rings always start in approximate rotational equilibrium. Gaseous satellites smear out along their specified orbits. Tori are initial models in pressure and rotational equilibrium.
[d] Ring inclination from the equatorial plane of the potential.
[e] Δr is the half thickness of the ring or the radius of the satellite, r is the radius of the pressure maximum or the middle of the ring/satellite.
[f] Ratio of the precession period to the rotation period.
[g] Polytropic index in the equation of state.
[h] Artificial viscosity is always added in SPH codes. The viscosity of the EH code is purely numerical and owes its existence to the differencing scheme. The viscosity in the "sticky-particle" code is due to cloud-cloud collisions.
[i] Is self-gravity important compared to the external potential?

small. Christodoulou & Tohline (1992) computed the evolution of the same torus in a potential with $c/a = 0.71$ (models 4). The strong quadrupole distortion forced the torus to move abruptly toward the preferred plane and simultaneously flow into the nuclear region after only a few rotations. Quinn (1991a) used a "sticky-particle" cloud-fluid code and found that once highly inclined rings form in a moderately triaxial potential, they can survive for many rotation periods close to their original inclination. An important feature of Quinn's simulations is that the rings, which form from initially orbiting ring segments, stay radially and vertically thin, substantially minimizing the effects of differential precession.

2.2. *New Computations and Results*

Katz & Rix (1992a, b) have recently used the TREESPH code to evolve a grid of models. Radiative cooling and self-gravity were also included in most of these simulations. We list only the models that are relevant for rings at high inclinations in Table 1 (models 5–7). They find that if cooling is included during the evolution of highly inclined rings inside oblate, scale-free, logarithmic potentials with $0.70 \lesssim c/a \lesssim 0.90$, the rings manage to find a somewhat warped, quasi-equilibrium state and survive for more than 30 rotations. The warp, which bends away from the poles, allows the entire ring to lock into solid-body precession, virtually eliminating differential precession, minimizing gas-gas collisions. For example, consider a spheroidal scale-free logarithmic potential of the form

$$\Phi(R, Z) = \frac{1}{2} v_0^2 \ln\left(\frac{R^2}{a^2} + \frac{Z^2}{c^2}\right), \qquad (1)$$

where v_0 is the rotation velocity of a zeroth-order circular orbit and (R, Z) are cylindrical coordinates. The precession frequency of an orbit is proportional to $r^{-1} \cos i$ where i is the inclination and r is the radius of the orbit (Steiman-Cameron & Durisen 1990). Therefore, a constantly precessing structure must obey the relation

$$\frac{\cos i}{r} = \text{constant}, \qquad (2)$$

i.e., the structure must be part of a circle in the (r, i)-plane with no vertical thickness. Models 5 and 7 closely follow relation (2) but gas-gas collisions are not completely eliminated because the ring still has some vertical thickness. Therefore, differential precession is expected to destroy the ring but only after many orbits (>30). Radiative cooling of the gas is crucial to keep the rings thin to delay the effects of differential precession. Of models starting from different initial conditions, either rings in centrifugal balance or accreted satellites entering the potential and then smearing out to form a ring after ~ 10 rotations, all manage to find the warped quasi-equilibrium state. However, if cooling is not included the rings collapse into the nucleus after only a few orbits (models 6).

If the scale-free, logarithmic potential is moderately prolate ($c/a = 1.33$), though, our recent TREESPH calculations show that the same rings collapse into the nucleus after only five rotations (model 10). Quinn (1991b; model 9 in Table 1) has confirmed this peculiar behavior of highly inclined rings inside moderately prolate potentials using his "sticky-particle" code. We have also obtained a similar result with the three-dimensional Eulerian hydro code for the evolution of a highly inclined toroidal equilibrium in a potential with $c/a = 1.33$ (model 11).

For this paper, we have evolved some additional models besides the moderately prolate ones mentioned above. They are listed at the bottom of Table 1. All these additional models started with a ring in centrifugal balance, i.e., in approximate equilibrium. To compare with Katz & Rix (1992a), we evolved rings in weakly oblate and prolate potentials using Habe's SPH code (models 12 and 13). The oblate model survived for more than 40 rotations but the prolate model was destroyed. We also evolved rings inside the same oblate, scale-free, logarithmic potentials of Katz & Rix (models 6) but using the three-dimensional Eulerian hydro code (models 14) and found that these rings shrink toward the nuclear region on time scales that decrease as the distortion of the potential is increased (from 15 to five orbits, see Table 1).

Finally, note that several of the models listed in Table 1 started with identical initial conditions but were evolved with different hydro codes. These models are 5 and 8 ($c/a = 0.75$), 9 and 10 ($c/a = 1.33$), and 6 and 14 ($c/a = 0.75$ and $c/a = 0.90$).

3. DISCUSSION OF RESULTS

3.1. *Difference between Oblate and Prolate Potentials*

The surprising difference between the evolution of highly inclined rings inside oblate and prolate potentials with moderate distortions requires an explanation. Recall that in oblate potentials the rings find constantly precessing, long-lived states while in prolate potentials the rings are violently unstable and collapse to the nucleus in a few orbits. Contrary to our initial expectations, it seems that the two geometries are not dynamically equivalent. The dynamical difference between the two potentials can be traced to the same effect that causes orbits in the two potentials to precess in different directions, i.e., the sign change of the quadrupole term between oblate and prolate potentials.

Consider a closed orbit inclined by an angle i to the equatorial plane of a spheroidal scale-free logarithmic potential. Furthermore, without loss of generality assume that the orbit intersects that plane on the x axis. By rotating the coordinate frame about the x-axis of the potential and using equation (1) we find that the gravitational force perpendicular to the plane of the orbit is

$$F_\perp = -\epsilon v_0^2 \frac{y \sin i \cos i}{r^2 + \epsilon y^2 \sin^2 i}, \qquad (3)$$

where $\epsilon = (a^2 - c^2)/c^2$, $y = r \sin \phi$, and (r, ϕ) are polar coordinates in the plane of the orbit. For an oblate potential $\epsilon > 0$ and $F_\perp < 0$ at the upper part of the orbit where $y > 0$. Similarly, for a prolate potential $\epsilon < 0$ and $F_\perp > 0$ for $y > 0$. At the points where the orbit intersects the equatorial plane of the potential $y = 0$ and $F_\perp = 0$. The net effect of this force is to tip the upper and lower extremes of the orbit toward the equatorial plane in an oblate potential and toward the polar plane in a prolate potential. Therefore, the ring is "warped" in the direction of the pseudo-equilibrium (eq. [2]) only inside an oblate potential. Note that this type of warping is achieved before precessional motions take over. In the oblate case, the constantly precessing configuration is established within less than one-third of a precession time and minimizes differential precession. In the prolate case, the ring begins to warp toward the polar plane in less than one-third of a precession time. This increases differential precession and the ring quickly collapses into the nucleus of the potential.

The difference in force direction, derived in equation (3), can be simply understood. Consider an inclined circular orbit inside a spheroidal potential. This orbit is defined by the zeroth-order, spherical term of the potential. In an oblate potential, the next higher order term of the potential, the quadrupole term, is equivalent to having excess mass in the equatorial plane. The uppermost and lowermost parts of the orbit are therefore attracted and tipped toward the equatorial plane of the potential. In a prolate potential, however, the quadrupole term is equivalent to having excess mass at the two poles of the potential. Now, the uppermost and lowermost parts of the orbit are attracted and tipped toward the poles of the potential.

All our SPH models in Table 1 support this explanation. The highly inclined rings clearly warp in different directions inside oblate and prolate potentials within 0.2 precession periods. This is clearly visible in Figure 1 which shows the contours of the projected surface density in models 5 and 10 after about 0.2 precession periods. Consistent with equation (3), only the ring in the oblate model warps in the direction specified by equation (2) and eventually achieves the long-lived, constant precession state. The ring in the prolate model warps toward the polar plane of the potential and quickly collapses into the nucleus. (This "symmetry breakdown" between oblate/prolate geometries reminds us of another well-known result: a potential tumbling about its short axis can support only a warped steady state only if the gas moves in retrograde orbits [see the review of Steiman-Cameron 1991 and the demonstration of Habe & Ikeuchi 1988].) Note that the pseudo-equilibrium state cannot be achieved at low and moderate inclinations in any type of potential because the large precession frequencies cause orbits to intersect frequently, forcing the gas to settle to the equatorial plane.

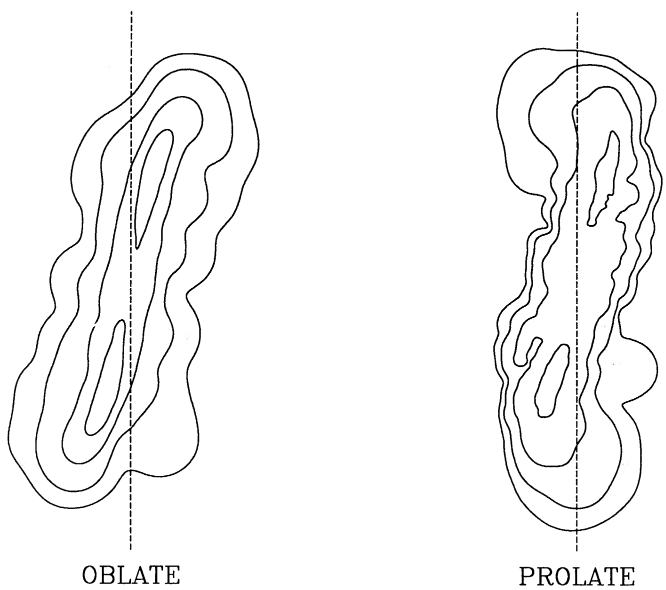

FIG. 1.—Two TREESPH simulations of rings inclined by 80° from the equatorial plane of an oblate and a prolate potential after ~ 0.2 precession periods. In both models, radiative cooling of the gas is included, self-gravity is negligible, and the radial thickness of the original ring is $\Delta r/r = 0.1$. The oblate model (5 in Table 1) has an axis ratio $c/a = 0.75$ and the prolate model (10 in Table 1) has $c/a = 1.33$. The dashed vertical lines denote the c axis of the potential. Contours of the logarithm of the projected density distributions clearly show that the two rings bend in opposite directions. Only the oblate model bends in the direction consistent with equation (2), necessary for constant precession. Note that the prolate model already appears substantially distorted.

3.2. *Nonequilibrium Initial Conditions*

The models evolved inside oblate potentials with cooling (models 5, 7, 8) or with nearly exact toroidal equilibria (defined by both pressure support and rotation; models 3) show that highly inclined rings can survive over long time scales inside oblate potentials. On the contrary, when cooling is not included, rings initially in only approximate centrifugal balance either settle significantly (model 2) or collapse into the nucleus of the potential (models 6, 14).

These differences can be traced to whether strong shocks occur and to how the different numerical techniques handle the shocks. For an adiabatic gas, shocks induce rapid evolution and collapse (see Katz & Rix 1992a) by increasing the heat content of the gas. Such shocks occur in nonequilibrium configurations (e.g., rings in approximate centrifugal balance) where the gas is cold compared to the virial temperature and collides at speeds comparable to the orbital velocity but they do not occur in nearly exact toroidal equilibria. In simulations without cooling, these shocks increase the thermal energy of the gas and the rings thicken. Once the ring is thickened, gas-gas collisions occur in directions both perpendicular to and in the ring plane owing to differential precession. All these gas-gas collisions lead to further shock heating, further thickening the ring until the gas finally virializes under strong inflow to conserve its z angular momentum. The relative importance of inflow and settling depends on the details of the numerical algorithm. In the simulations that include cooling, the shock energy is radiated away on time scales that are much shorter than a dynamical time so the gas remains essentially isothermal. As long as the gas remains much colder than the virial temperature the ring can remain thin and retain its identity.

Thus the simulations without cooling can only be expected to agree in detail when strong shocks are not present at early stages of the evolution. The TREESPH models with cooling avoid this sensitivity; starting from diverse initial conditions inside oblate potentials, they always find the long-lived, constantly precessing state at high inclinations. In contrast, the Eulerian hydro code models, if started away from their good quality equilibrium, quickly collapse to the nucleus of the potential owing to the limited spatial resolution and lack of cooling.

3.3. *Influence of Viscosity*

A final issue that needs to be clarified is the role of viscosity in the above results. Information about the viscosity used by various investigators and some related references are listed in Table 1. Steiman-Cameron & Durisen (1988) and Christodoulou & Tohline (1992) argued that, although some viscous mechanism is necessary for settling to occur, the dependence of the evolution time scales on the magnitude and type of viscosity is weak. Our recent calculations confirm this point; all three hydro codes use artificial viscosities of different types and magnitudes. However, Varnas (1990) argues against this viewpoint. We question this disagreement, especially since his quantitative results confirm the original results of Steiman-Cameron & Durisen (1988), that, for low and moderate inclinations, the settling time scales as (viscosity coefficient)$^{-1/3}$. Specifically, Varnas found for a ring originally inclined by 30°

that changing the artificial viscosity parameter α by a factor of 10 results in settling times that differ by only a factor of ~ 2.

4. EVOLUTIONARY SCENARIOS

From the models that we have compared above we have reached the following concensus for the evolution of galactic rings at high inclinations (typically 80°) with respect to the equatorial plane of a static, spheroidal halo.

1. If the external potential does not deviate much from spherical symmetry, i.e., the axis ratio obeys $0.9 \lesssim c/a \lesssim 1.1$, then differential precession and dissipation time scales are very long. The ring is expected to survive close to the original inclination without settling significantly. Some inflow of matter toward the nuclear region is also expected but the effect on the ring is minor. In an attempt to reduce differential precession, the ring will not remain flat but will assume a somewhat warped structure, assisted by continuous cooling of the gas (Katz & Rix 1992a; see also Quinn 1991a). If cooling is not efficient, then a weak warp will still develop as the ring manages to settle slowly by a few degrees. Only this scenario is in good qualitative agreement with the theoretical prediction that time scales for differential precession and settling are very long at high inclinations.

2. For moderate oblate distortions in the potential ($0.7 \lesssim c/a \lesssim 0.9$) and if cooling is efficient, the calculations of Katz & Rix (1992a) provide a mechanism that still preserves the ring for many orbits: cooling helps the ring develop a stable warp and survive over long time scales. The warp adjusts itself so that the precession frequency at all radii is equal, thus reducing gas-gas collisions. Typically, rings survive for more than 30 orbits, the duration of the entire computation, which is longer than one Hubble time for many observed polar rings. This scenario will have to be invoked to explain the longevity of nearly massless polar rings inside moderately distorted, oblate halos. An important signature of such highly inclined rings is that they should always warp away from the polar orientation (cf. the polar-ring galaxies UGC 5600 and NGC 2685; see Sackett 1991).

3. If the external potential is strongly oblate in shape (say, $c/a \ll 0.7$), then a slow, gradual evolution of the ring cannot be anticipated, even with the stabilizing influence of radiative cooling. The primary effect of the strong quadrupole perturbation is to accelerate the overall evolution, making it abrupt and violent (Christodoulou & Tohline 1992). The dynamical time scale becomes competitive with the cooling time scale. Although very prominent warps form, they are transient and last only a few rotations. As settling drives the ring quickly out of equilibrium, matter inflow becomes very important and the central hole is flooded with gas in only a few rotations. Because of the short duration of the evolution, such distorted disk structures probably cannot be observed. Some of the nuclear disks observed in galaxies and the irregular morphology of some galaxies may, however, be the results of this evolutionary scenario.

4. If the external potential is distinctly prolate spheroidal ($c/a \gtrsim 1.2$), then the ring begins to disrupt after only about five orbits. This behavior of highly inclined rings inside prolate potentials runs contrary to the common intuition that oblate and prolate halos are dynamically equivalent. The transient but long-lived, constant-precession state inside a prolate potential cannot be achieved because in this state the gas must warp toward lower inclinations (i.e., away from the poles, see eq. [2]) while the component of the gravitational force perpendicular to the ring keeps tipping the orbiting gas toward higher inclinations (see eq. [3]). This scenario does not depend on the quality of the initial equilibrium or the gas cooling efficiency (see, e.g. Habe & Ikeuchi 1985).

In this work we have not excluded the possibility of stable models of polar rings that are based on the effects of self-gravity or the triaxiality of the potential. But we do believe that many of the polar rings observed in galaxies (Schweizer, Whitmore, & Rubin 1983; Whitmore, McElroy, & Schweizer 1987; Whitmore et al. 1990) can be understood "to zeroth order" without complicating the hydrodynamical models with elaborate features, such as strong self-gravity of the ring, figure rotation, or triaxiality of the potential. The following possible exceptions are, however, noted: (a) the dust-lane elliptical NGC 5266 where retrograde tumbling of a triaxial potential might be required (Varnas et al. 1987); (b) the polar-ring galaxy NGC 4650A where the ring might be massive and the potential might be substantially distorted (Sackett & Sparke 1990); and (c) the two-ring structure of the "helix" galaxy NGC 2685 where self-gravity may play an important role (Peletier & Christodoulou 1992). Our results show that highly inclined rings in galaxies can survive comfortably for many orbits (>30) inside weakly spheroidal or even moderately oblate halos (scenario 1 and 2, respectively), while the detailed observations of polar-ring galaxies do not clearly demonstrate and possibly argue against the existence of either strongly distorted (scenario 3) or distinctly prolate (scenario 4) halos.

Computations have been carried out on the following machines: the IBM 3090 of the IBM Research Center, Palo Alto, CA; the Cray Y-MP of the San Diego Supercomputer Center; the Cray Y-MP of the Pittsburgh Supercomputer Center; and the HITAC S-820/80 of the Hokkaido University. D. M. C. is currently supported by a Presidential Young Investigator Award (AST 91-48279) from the National Science Foundation awarded to Ramesh Narayan. N. K. is supported by a Hubble Space Telescope fellowship. H. W. R. is supported by a grant (AST 88-22297) from the National Science Foundation awarded to Simon White and a Hubble Space Telescope fellowship. A. H. is supported by the Grant-in-Aid 01540209 of the Japanese Ministry of Education, Science, and Culture.

REFERENCES

Athanassoula, E., & Bosma, A. 1985, ARA&A, 23, 147
Christodoulou, D. M. 1989, Ph.D. thesis, Louisiana State Univ.
———. 1990, in Ann. NY Acad. Sci. No. 596, Galactic Models, ed. J. R. Buchler, S. T. Gottesman, & J. H. Hunter, Jr., 207
Christodoulou, D. M., & Tohline, J. E. 1991, in Warped Disks and Inclined Rings around Galaxies, ed. S. Casertano, P. Sackett, & F. Briggs (New York: Cambridge Univ. Press), 122
———. 1992, ApJ, submitted
Durisen, R. H., Tohline, J. E., Burns, J. A., & Dobrovolskis, A. R. 1983, ApJ, 264, 392
Habe, A., & Ikeuchi, S. 1985, ApJ, 289, 540
———. 1988, ApJ, 326, 84
Hernquist, L., & Katz, N. 1989, ApJS, 70, 419
Katz, N., & Rix, H.-W. 1992a, ApJ, 389, L55
———. 1992b, ApJ, in preparation
Peletier, R., & Christodoulou, D. M. 1992, AJ, submitted
Quinn, T. 1991a, in Warped Disks and Inclined Rings around Galaxies, ed. S. Casertano, P. Sackett, & F. Briggs (New York: Cambridge Univ. Press), 143
———. 1991b, private communication

Rix, H.-W., & Katz, N. 1991, in Warped Disks and Inclined Rings around Galaxies, ed. S. Casertano, P. Sackett, & F. Briggs (New York: Cambridge Univ. Press), 112
Sackett, P. D. 1991, in Warped Disks and Inclined Rings around Galaxies, ed. S. Casertano, P. Sackett, & F. Briggs (New York: Cambridge Univ. Press), 73
Sackett, P. D., & Sparke, L. S. 1990, ApJ, 361, 408
Schechter, P. L., & Gunn, J. E. 1978, AJ, 83, 1360
Schweizer, F., Whitmore, B. C., & Rubin, V. C. 1983, AJ, 88, 909
Steiman-Cameron, T. Y. 1991, in Warped Disks and Inclined Rings around Galaxies, ed. S. Casertano, P. Sackett, & F. Briggs (New York: Cambridge Univ. Press), 131
Steiman-Cameron, T. Y., & Durisen, R. H. 1982, ApJ, 263, L51
———. 1984, ApJ, 276, 101
Steiman-Cameron, T. Y., & Durisen, R. H. 1988, ApJ, 325, 26
———. 1990, ApJ, 357, 62
Tohline, J. E. 1990, in Ann. NY Acad. Sci. No. 596, Galactic Models, ed. J. R. Buchler, S. T. Gottesman, & J. H. Hunter, Jr., 198
Tohline, J. E., & Durisen, R. H. 1982, ApJ, 257, 94
Tohline, J. E., Simonson, G. F., & Caldwell, N. 1982, ApJ, 252, 92
Varnas, S. R. 1986a, Ph.D. thesis, Monash Univ.
———. 1986b, Proc. Astron. Soc. Australia, 6, 458
———. 1990, MNRAS, 247, 674
Varnas, S. R., Bertola, F., Galletta, G., Freeman, K. C., & Carter, D. 1987, ApJ, 313, 69
Whitmore, B. C., Lucas, R. A., McElroy, D. B., Steiman-Cameron, T. Y., Sackett, P. D., & Olling, R. P. 1990, AJ, 100, 1489
Whitmore, B. C., McElroy, D. B., & Schweizer, F. 1987, ApJ, 314, 439